

RESEARCH ARTICLE

Open Access



Prognostic and predictive value of interstitial lung abnormalities and EGFR mutation status in patients with non-small cell lung cancer

Xiaoli Xu¹, Min Zhu², Zixing Wang³, Jialu Li¹, Tao Ouyang¹, Cen Chen⁴, Kewu Huang², Yuhui Zhang^{2*} and Yanli L. Gao^{1,2*} 

Abstract

Background To determine the predictive value of interstitial lung abnormalities (ILA) for epidermal growth factor receptor (EGFR) mutation status and assess the prognostic significance of EGFR and ILA in patients with non-small cell lung cancer (NSCLC).

Methods We reviewed 797 consecutive patients with a histologically proven diagnosis of primary NSCLC from January 2013 to October 2018. Of these, 109 patients with NSCLC were found to have concomitant ILA. Multivariate logistic regression analysis was used to identify the significant clinical and computed tomography (CT) findings in predicting EGFR mutations. Cox proportional hazard models were used to identify significant prognostic factors.

Results EGFR mutations were identified in 22 of 109 tumors (20.2%). Multivariate analysis showed that the models incorporating clinical, tumor CT and ILA CT features yielded areas under the receiver operating characteristic curve (AUC) values of 0.749, 0.838, and 0.849, respectively. When combining the three models, the independent predictive factors for EGFR mutations were non-fibrotic ILA, female sex, and small tumor size, with an AUC value of 0.920 (95% confidence interval[CI]: 0.861–0.978, $p < 0.001$). In the multivariate Cox model, EGFR mutations (hazard ratio = 0.169, 95% CI = 0.042–0.675, $p = 0.012$; 692 days vs. 301 days) were independently associated with extended overall survival compared to the wild-type.

Conclusion Non-fibrotic ILA independently predicts the presence of EGFR mutations, and the presence of EGFR mutations rather than non-fibrotic ILA serves as an independent good prognostic factor for patients with NSCLC.

Keywords X-ray computed tomography, Lung cancer, EGFR, Interstitial lung abnormality, Overall survival

*Correspondence:

Yuhui Zhang
zhangyhcy@163.com

Yanli L. Gao
radiologygaoyanli@163.com

¹ Department of Radiology, Beijing Chao-Yang Hospital, Capital Medical University, No. 8 Gongtinan Road, Beijing 100020, China

² Department of Pulmonary and Critical Care Medicine, Beijing Institute of Respiratory Medicine, Beijing Chao-Yang Hospital, Capital Medical University, No. 8 Gongtinan Road, Beijing 100020, China

³ Institute of Basic Medical Sciences, School of Basic Medicine, Chinese Academy of Medical Sciences, Peking Union Medical College, Beijing, China

⁴ Department of Radiology, Beijing Nuclear Industry Hospital, Beijing, China



© The Author(s) 2024. **Open Access** This article is licensed under a Creative Commons Attribution 4.0 International License, which permits use, sharing, adaptation, distribution and reproduction in any medium or format, as long as you give appropriate credit to the original author(s) and the source, provide a link to the Creative Commons licence, and indicate if changes were made. The images or other third party material in this article are included in the article's Creative Commons licence, unless indicated otherwise in a credit line to the material. If material is not included in the article's Creative Commons licence and your intended use is not permitted by statutory regulation or exceeds the permitted use, you will need to obtain permission directly from the copyright holder. To view a copy of this licence, visit <http://creativecommons.org/licenses/by/4.0/>. The Creative Commons Public Domain Dedication waiver (<http://creativecommons.org/publicdomain/zero/1.0/>) applies to the data made available in this article, unless otherwise stated in a credit line to the data.

Introduction

Interstitial lung abnormalities (ILAs) are increasingly recognized and identified in populations screened for lung cancer, with studies reporting their presence in 4–10% of cigarette smokers undergoing lung cancer screening [1–3], making them an important comorbidity in patients with lung cancer. According to the Fleischner Society, ILAs are radiological abnormalities incidentally detected on chest computed tomography (CT) in patients without a history of interstitial lung disease (ILD) with the potential for progression to idiopathic pulmonary fibrosis (IPF) or other fibrotic ILDs [1, 4]. Multiple large cohort studies have demonstrated a correlation between ILAs and an elevated incidence of lung cancer, heightened risk of all-cause mortality, and increased pulmonary complications associated with cancer treatment in patients [2, 5, 6]. Therefore, it is important to fully elucidate the relationship between ILAs and lung cancer before administering treatment in clinical practice.

With an increasing understanding of the molecular mechanisms underlying lung cancer, the treatment approach for non-small cell lung cancer (NSCLC) has evolved to prioritize the identification of specific oncogenic driver mutation subtypes, especially epidermal growth factor receptor (EGFR) mutations, which are the most common gene mutations and indicate longer overall survival for patients with NSCLC [7, 8]. Detection of EGFR mutation status typically requires invasive sampling of tumor tissue by surgery or biopsy. Inspired by genomics and tumor heterogeneity, thorough data mining of CT images has the potential to improve clinical decision-making [9]. Studies have demonstrated that the CT features of tumors could help identify the EGFR mutation status in patients [9–11]. A low prevalence of EGFR mutations has been previously reported in patients with lung cancer with usual interstitial pneumonia (UIP) [12]. However, the correlation between CT features of ILAs and EGFR mutations in NSCLC with coexisting ILAs has not yet been fully elucidated.

Studies have reported that patients with lung cancer and ILAs exhibit a lower 5-year overall survival (OS) rate than patients without ILA, yet demonstrate a higher 5-year OS rate than patients with IPF, and both fibrotic and non-fibrotic components of ILAs are associated with poor OS in patients with operable lung cancer [13, 14]. Nevertheless, there is a scarcity of studies that have concurrently examined EGFR mutations and ILAs in the assessment of prognosis among patients with lung cancer, particularly those in advanced stages. Hence, the objective of this study was to conduct a retrospective analysis of the predictive capability of ILA features on CT images for EGFR mutations, and to assess the prognostic

significance of ILA and EGFR mutation status in patients with NSCLC with concurrent ILAs.

Methods

Study population

The Ethics Committees of Beijing Chao-Yang Hospital, Capital Medical University (no. 2021-ke-443) approved this retrospective, single-center study and waived the requirement for informed consent. A total of 797 consecutive patients with a histologically proven diagnosis of primary NSCLC underwent chest high-resolution CT (HRCT) between January 2013 and October 2018 at our hospital. The exclusion criteria were as follows: (i) previous thoracic surgery, radiation therapy, or chemotherapy; (ii) severe tuberculosis or pneumoconiosis; (iii) history of collagen vascular disease; (iv) preexisting ILD; and (v) missing clinical data. The HRCT images of these patients were reviewed retrospectively by two pulmonary radiologists (X-L X and Y-L G, with 10 and 25 years of experience, respectively) to identify the radiological evidence of concomitant ILA. According to the criteria of the Fleischner Society, ILAs are diagnosed as non-dependent ground-glass opacities (GGO), reticular abnormalities, architectural distortion, non-emphysematous cysts, honeycombing, and traction bronchiectasis that affect >5% of any lung zone [4, 15]. Finally, 109 patients with concomitant lung cancer and ILA were included in this study (Fig. 1). Histological diagnosis was based on the World Health Organization classification published in 2021 [16] and TNM staging of lung cancer was according to the eighth edition [17], respectively. Molecular analysis of the EGFR mutation status was performed using polymerase chain reaction-based amplification-refractory mutation system analysis with the Human EGFR Gene Mutations Detection Kit (Beijing ACCB Biotech, Beijing, China). Smoking status was determined by reviewing medical records and was quantified by pack-years.

CT evaluation by radiologists

CT images were obtained for all patients in the supine position at the end of inspiration using a variety of CT units. Images were reconstructed with contiguous 1–2 mm sections using a high-resolution reconstruction algorithm for analysis. Two chest radiologists independently evaluated the CT images in random order without any clinical or pathologic information. Image analysis was performed using the indicated window settings (lung: width, 1500 HU; level, -400 HU; mediastinum: width, 400 HU; level, 40 HU) for axial images on a picture archiving and communication system; radiologists were allowed to moderately change the default window settings for ease of assessment.

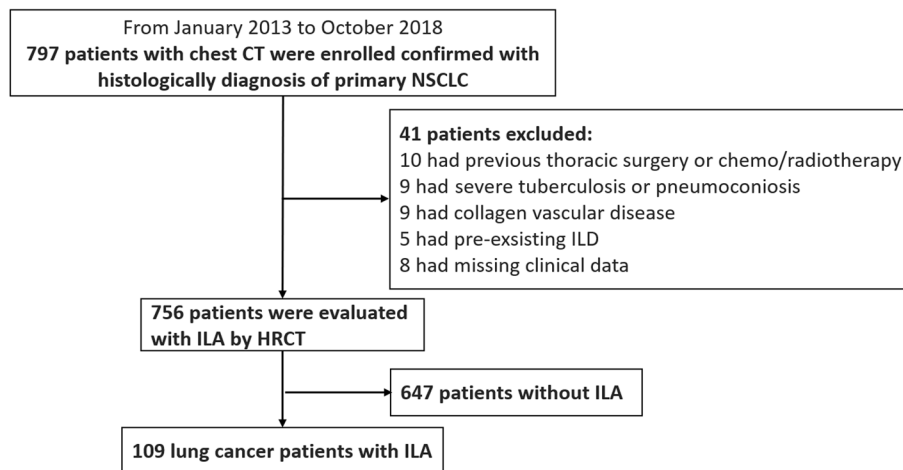


Fig. 1 Flowchart of the selection of the study population and the exclusion criteria. CT, computed tomography; HRCT, high-resolution CT; ILA, interstitial lung abnormality; ILD, interstitial lung disease; NSCLC, non-small cell lung cancer

ILAs were subcategorized as non-subpleural, subpleural nonfibrotic, and subpleural fibrotic ILA [4], with subpleural fibrotic ILA corresponding to a probable usual interstitial pneumonia pattern [18]; non-subpleural ILA and subpleural nonfibrotic ILA were defined as non-fibrotic ILA in this study. The distribution, overall extent of the lesions, and extent of each ILA lesion were further evaluated, and disagreements concerning the scores were resolved by consensus. The predominant distribution included peripheral, peribronchovascular, and mixed patterns. The extent of CT findings of ILA in each case was scored using a four-point scale (score of 1, 5–25% involvement; score of 2, 26–50% involvement; score of 3, 51–75% involvement; and score of 4, 76–100% involvement) [1]. The extent of the ILA findings was further assessed in six lung zones (upper, middle, and lower zones of both lungs) on CT images. The division of the upper, middle, and lower lung zones was determined based on the levels of the inferior aortic arch and right inferior pulmonary vein [4]. Readers scored the lung fields that showed abnormalities in each of the six zones based on GGO, reticulation, and honeycombing. The average of the six lung zones was used to calculate the percentage of the whole lungs. Traction bronchiectasis was assessed by summing the number of bronchiectasis-affected pulmonary segments [19].

Morphological CT features of lung tumors were also analyzed, including location, size (maximum long-axis diameter), shape (round, somewhat irregular, irregular), density (solid, part-solid, GGO), margin (lobulation, spiculation), internal (vacuole sign, lumen, cavity, air bronchogram, bronchial cut-off sign), surrounding structures (vascular convergence, pleural traction, halo sign), and associated findings (pleural fluid). Previously published

evaluation methods were used in this analysis [10, 20]. Disagreements regarding the CT features of lung cancer were resolved by consensus.

Statistical analysis

All statistical analyses were performed using SPSS version 20.0. Data are presented as means, medians, counts, and percentages, where appropriate. Clinical and CT feature variables between the EGFR mutation and wild-type groups were compared using X^2 or Fisher's test, Student's t-test, or the Mann–Whitney U test, where appropriate. Multiple logistic regression analysis was used to assess the value of clinical features, tumor CT findings, and ILA CT features in predicting EGFR mutations. Significant factors in the univariate analysis were identified as potential covariates in a multivariate logistic regression model using the forward likelihood ratio test. A receiver operating characteristic (ROC) curve was used to estimate the significant predictors of EGFR identification. The area under the curve (AUC) was calculated to determine the predictive capability. A *p* value of less than 0.05 was considered to indicate a significant difference.

The probabilities of OS at three and five years after diagnosis were estimated using the Kaplan–Meier method. Multivariate analysis was performed using the Cox proportional hazards model to evaluate the hazard ratios (HR) for OS probabilities with 95% confidence intervals (CI).

Results

Correlation of EGFR mutation status with clinical characteristics

The clinical features of the patients are shown in Table 1. EGFR mutations were identified in 22 of the 109 tumors

Table 1 Association between Clinical features and EGFR mutation status

Characteristic	Total	EGFR (+)	EGFR (-)	P value
No. of patients	109	22 (20.18)	87 (79.82)	
Sex				
Male	83 (76.15)	8 (36.36)	75 (86.21)	< 0.001
Female	26 (23.85)	14 (63.64)	12 (13.79)	
Age (y)^a	66.07 ± 8.14	64.82 ± 7.04	66.39 ± 8.41	0.421
Smoking history				< 0.001
Never a smoker	37 (33.94)	15 (68.18)	22 (25.29)	
Smoker	72 (66.06)	7 (31.82)	65 (74.71)	
Smoking amount (pack-year)^b	25(0,45)	0(0,25)	30(0,45)	0.007
Histologic finding				0.007
Adenocarcinoma	78 (71.56)	21 (95.45)	57 (65.52)	
Squamous cell carcinoma	27 (24.77)	1 (4.55)	26 (29.88)	
Others	4 (3.67)	0 (0)	4 (4.60)	
TNM staging				0.034
I + II	21(19.27)	8 (36.36)	13 (14.94)	
III + IV	88 (80.73)	14 (63.64)	74 (85.06)	
Diagnostic technique				
Surgery	24 (22.02)	11 (50)	13 (14.94)	
CT-guided biopsy	82 (75.23)	11 (50)	71 (81.61)	
others	3 (2.75)	0 (0)	3 (3.45)	

Unless otherwise indicated, data are numbers of patients, with the percentages in parentheses

EGFR Epidermal growth factor receptor

^a Data are means ± standard deviations

^b Data are the median with interquartile range in parentheses

(20.2%). EGFR mutations were more frequently observed in women (63.64%) than in men (36.36%) ($p < 0.001$), and in non-smokers (68.18%) than in smokers (31.82%) ($p < 0.001$). No difference in the average age was observed between the EGFR mutant and wild-type groups ($p = 0.421$). Most EGFR mutations (95.45%) were found adenocarcinomas ($p = 0.007$). Lung cancers with EGFR mutations mostly presented with an early TNM stage ($p = 0.034$).

Correlation of EGFR mutation status with CT features of ILA and tumors

The CT features of the ILA included in the univariate analysis for prediction of EGFR mutations are presented in Table 2. EGFR mutation rates were significantly lower in subpleural fibrotic ILA than in non-fibrotic ILA ($p < 0.001$) (Figs. 2 and 3). The ILAs in the EGFR mutant group were less distributed in the subpleural zone. The scores for reticulation in every zone and honeycombing in the middle and lower zones of the EGFR mutant group were significantly lower than those of the wild-type group. The degree of traction bronchiectasis was also less in the EGFR mutant group ($p < 0.001$). No significant

difference was noted in the GGO score of any lung zone between the EGFR mutant and wild-type groups.

Regarding the CT features of the lung tumors (Table 3), the tumor diameter of the EGFR mutation group was significantly smaller than that of EGFR wild-type group ($p < 0.001$). Spiculation ($p = 0.043$) and pleural traction ($p = 0.001$) were more frequently observed in the EGFR mutant group than in the wild type group, whereas pleural fluid was less frequently observed in the EGFR mutant group. In addition, tumors located in ILA had a lower rate of EGFR mutations ($p < 0.001$). Other CT features, such as location, shape, density, vacuole sign, lumen, cavity, air bronchogram, bronchial cutoff sign, lobulation, vascular convergence, and halo sign, showed no significant differences between the two groups.

Multivariable analysis and receiver operating characteristic curve analysis

In the multivariate analysis, for the model with clinical features, sex (OR = 0.091, 95% CI: 0.032–0.264; $p < 0.001$) was an independent predictive factor for the presence of EGFR mutations after adjusting for smoking history, histologic findings, and TNM staging, with an AUC value of 0.749 (95% CI: 0.622–0.877, $p < 0.001$). The model with

Table 2 CT Findings of ILA and Their Association with EGFR mutation

Estimation of extent	EGFR (+)	EGFR (-)	Pvalue
Subcategories	22	87	<0.001
Subpleural fibrotic ILA	2 (9.10)	55 (63.22)	
Subpleural nonfibrotic ILA	10 (45.45)	18 (20.69)	
Non-subpleural ILA	10 (45.45)	14 (16.09)	
Total score^a	1.23±0.53	1.28±0.48	0.580
Distribution			0.012
Subpleural	17 (77.27)	79 (90.80)	
Peribronchovascular	5 (22.73)	3 (3.45)	
Mixed	0	5 (5.75)	
Score of ILA findings^a			
Upper GGO	4.11±9.90	4.01±6.80	0.154
Middle GGO	7.61±10.41	10.13±10.98	0.068
Lower GGO	14.89±14.06	17.23±15.41	0.433
Upper reticulation	2.61±6.70	7.99±9.19	<0.001
Middle reticulation	3.75±4.41	12.66±11.67	<0.001
Lower reticulation	8.11±6.45	19.53±15.32	<0.001
Upper honeycombing	0.00±0.00	1.28±3.63	0.068
Middle honeycombing	0.11±0.53	2.83±5.67	0.001
Lower honeycombing	0.41±1.46	7.50±12.56	<0.001
Tractive bronchiectasis	1.91±3.90	7.15±5.46	<0.001

Unless otherwise indicated, data are numbers of patients, with the percentages in parentheses

ILA Interstitial lung abnormality, EGFR Epidermal growth factor receptor

^a Data are means ± standard deviations

tumor CT features showed that tumor located in ILA (OR=0.156, 95% CI: 0.046–0.529; $p=0.003$) and tumor diameter (OR=0.592, 95% CI: 0.415–0.846; $p=0.004$) were independent predictors of EGFR mutation; the corresponding AUC value was 0.838 (95% CI: 0.754–0.922, $p<0.001$). The model with ILA CT features indicated that subpleural fibrotic ILA (OR=0.097, 95% CI: 0.019–0.483; $p=0.004$) and middle reticulation (OR=0.890, 95% CI: 0.803–0.987; $p=0.027$) were independent predictors of EGFR mutations, with an AUC value of 0.849 (95% CI: 0.768–0.930, $p<0.001$). When combining the three models, the significantly independent predictors for EGFR mutation were subpleural fibrotic ILA (OR=0.169, 95% CI: 0.030–0.964; $p=0.043$), sex (OR=0.141, 95% CI: 0.035–0.557; $p=0.005$) and tumor diameter (OR=0.637, 95% CI: 0.429–0.944; $p=0.025$), giving a predictive value for EGFR mutations with the AUC value of 0.920 (95% CI: 0.861–0.978, $p<0.001$), a diagnostic sensitivity of 90.9% and a specificity of 86.2% (Fig. 4).

The Kaplan–Meier curves for OS based on EGFR status are shown in Fig. 5. Patients with EGFR mutations had a longer OS than those without EGFR mutations

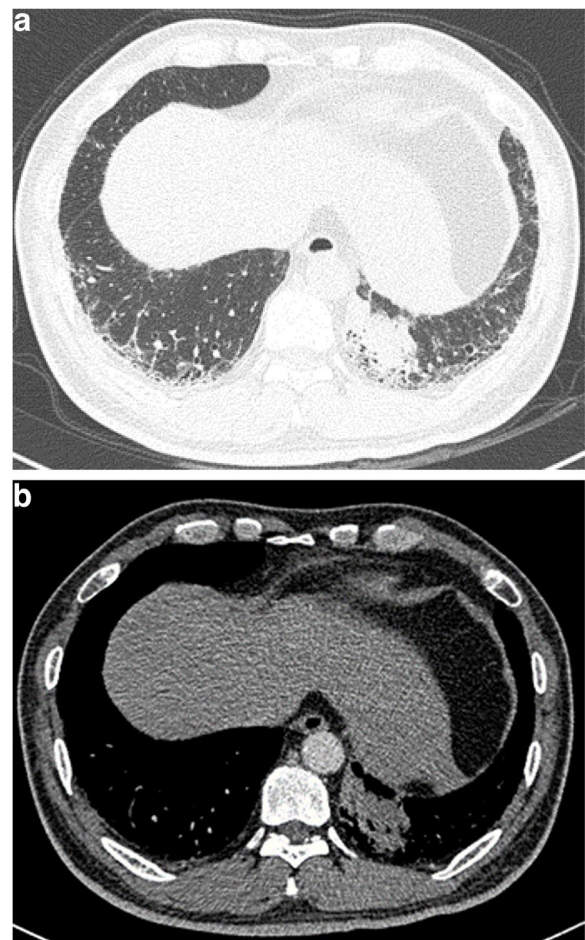


Fig. 2 A 54-year-old male smoker with stage IV adenocarcinoma located in the left lower lobe. Pre-treatment chest CT (a) demonstrated ground-glass opacity, reticulation, traction bronchiectasis, and honeycombing predominantly located in bilateral lower lobes, in accordance with subpleural fibrotic ILA. The tumor was located in ILAs and presented the lobulation sign (a, b). The patient underwent fine needle aspiration biopsy, with a pathological diagnosis of adenocarcinoma without EGFR mutation. He was died 300 days after the diagnosis of lung cancer. CT, computed tomography

($p<0.001$). In the univariate analysis of OS after diagnosis, sex, smoking status, subpleural fibrotic ILA, EGFR status, TNM staging, histologic findings, pleural traction, and presence of pleural fluid were predictive factors. In the multivariate analysis, EGFR mutation (HR=0.169, 95% CI=0.042–0.675, $p=0.012$; 692 days vs. 301 days), TNM stage III–IV (HR=14.819, 95% CI=1.936–113.407, $p=0.009$; 336 days vs. 580 days), and presence of pleural fluid (HR=2.796, 95% CI=1.347–5.803, $p=0.006$; 274 days vs. 489 days) were independent prognostic factors for OS (Table 4).

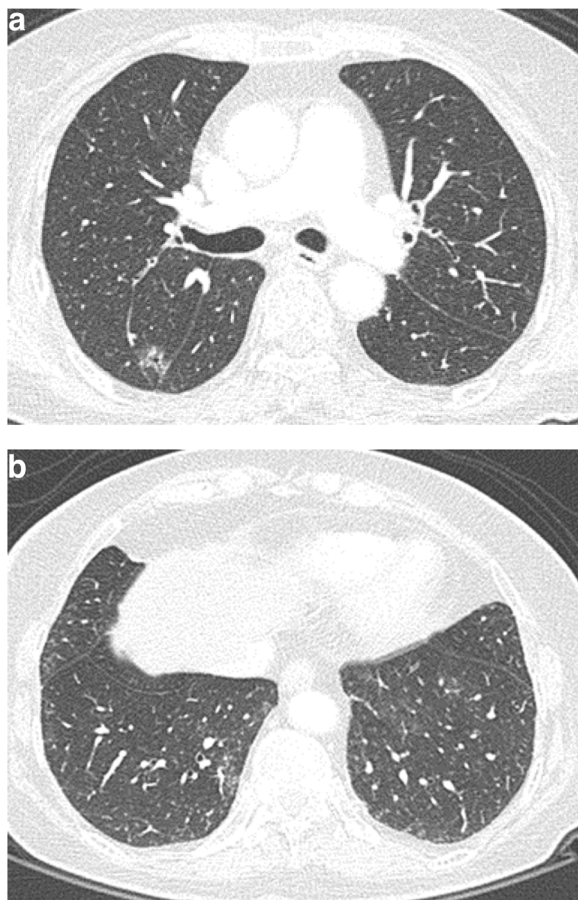


Fig. 3 A 69-year-old female nonsmoker with stage I adenocarcinoma located in the right upper lobe. Pre-treatment chest CT demonstrated the tumor with signs of lobulation, spiculation, vacuole and pleural traction (a). Ground-glass opacity and reticulation were observed in bilateral lower lobes without subpleural predominance, in accordance with non-fibrotic ILA (b). The patient underwent surgery, and a pathological diagnosis of adenocarcinoma with EGFR mutation was made. She was still alive at the end of follow-up. CT, computed tomography

Table 3 CT Findings of tumor and their association with EGFR

Estimation of tumor	EGFR (+)	EGFR (-)	P value
Diameter(cm) ^a	3.10 ± 1.15	5.26 ± 2.62	< 0.001
Spiculation (+)	19(86.36)	55(63.22)	0.043
Pleural traction (+)	19(86.36)	41(47.13)	0.001
Pleural fluid (+)	6(27.27)	48(55.17)	0.030
Tumor located in ILA	4(18.18)	54(62.07)	< 0.001

Unless otherwise indicated, data are numbers of patients, with the percentages in parentheses

EGFR Epidermal growth factor receptor, ILA Interstitial lung abnormality

^a Data are means ± standard deviations

Discussion

The evaluation of EGFR mutations and associated risk factors of OS in patients with NSCLC is crucial for

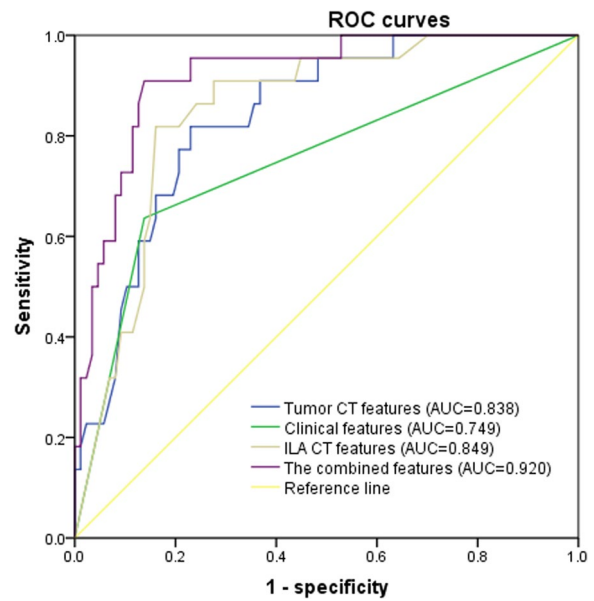
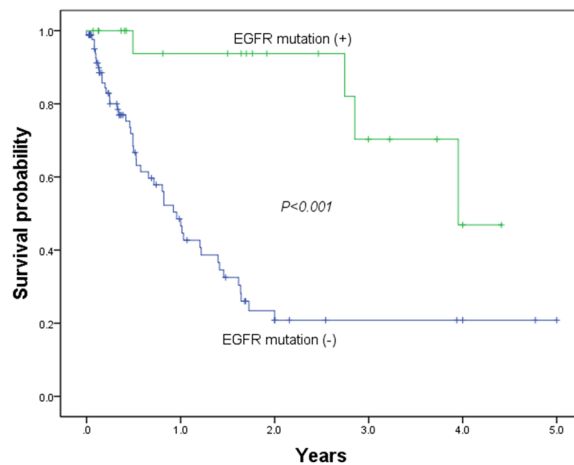


Fig. 4 Receiver operating characteristic curves applied to predict EGFR mutation status. The curves are shown for models based on clinical features, tumor CT features, ILA CT features and integrated features. AUC, area under the ROC curve; CT, computed tomography; EGFR, epidermal growth factor receptor; ILA, interstitial lung abnormality; ROC, receiver operating characteristic

clinicians to determine the appropriate course of treatment, monitor treatment efficacy, and predict patient outcomes. Previous investigations have revealed an unfavorable prognosis for ILA in patients with lung cancer [13, 14, 21, 22]. Our previous study comprehensively analyzed the prevalence of ILAs, clinical characteristics, and prognosis of patients with newly diagnosed NSCLC [22]. Based on this foundation, in this study we have expanded the investigation into the subgrouping of ILAs through CT analysis, exploring their potential predictive value for determining the EGFR status of tumors and long-term prognosis. This showed that the CT features of ILAs were predictive of the EGFR mutation status, and the combined clinical and imaging features could further improve the predictive ability for EGFR mutation status. The OS was shorter when patients with lung cancer presented with TNM stage III–IV, EGFR wild-type mutation, and pleural fluid. Moreover, non-fibrotic ILA was identified as an independent predictor of EGFR but not as independent prognostic factor for OS.

EGFR mutations have been observed at different rates in American and Asian populations, ranging from 28% in American non-smokers to 68% in Asian non-smokers [23]. This study found that the EGFR mutation rate was 20.2% in a Chinese population with lung cancer and coexistent ILA, and the mutation frequency in patients with subpleural fibrotic ILA (3.5%) was lower



Patients at risk

EGFR mutation	86	72	8	4	2	0
EGFR wild-type	21	14	9	5	1	0

Fig. 5 Overall survival according to the EGFR mutation status. The log-rank test showed that patients with EGFR mutations had a good overall survival compared to patients without EGFR mutations ($p < 0.001$). EGFR, epidermal growth factor receptor

Table 4 Univariate and multivariate Cox analysis for overall survival

Variables	Univariate analysis for OS		Multivariate analysis for OS	
	HR (95% CI)	P value	HR (95% CI)	P value
Sex (male vs. female)	3.066 (1.366–6.884)	0.007	1.091 (0.367–3.243)	0.875
Smoking status (current or former smoker vs. never)	2.121 (1.101–4.087)	0.025	1.384 (0.595–3.220)	0.450
ILA subcategory (subpleural fibrotic ILA vs. non-fibrotic ILA)	2.065 (1.156–3.690)	0.014	1.282 (0.678–2.424)	0.444
EGFR status (mutated vs. wild)	0.165 (0.059–0.466)	0.001	0.169 (0.042–0.675)	0.012
TNM staging (III-IV vs. I-II)	16.414 (2.258–119.292)	0.006	14.819 (1.936–113.407)	0.009
Histologic findings (adenocarcinoma vs. non-adenocarcinoma)	0.301 (0.156–0.581)	<0.001	0.612 (0.293–1.281)	0.193
Pleural traction (+)	0.503 (0.285–0.889)	0.018	0.802 (0.428–1.503)	0.491
Pleural fluid (+)	3.740 (2.005–6.977)	<0.001	2.796 (1.347–5.803)	0.006

OS Overall survival, HR Hazard ratio, CI Confidence interval, EGFR Epidermal growth factor receptor, ILA Interstitial lung abnormality

than that in those with non-fibrotic ILA (38.5%), which is similar to findings in earlier studies in the Japanese population [12, 24]. Although some researchers have reported a high risk of acute exacerbation caused by molecular-targeted agents among patients with lung cancer and coexisting ILD [25, 26], tyrosine kinase inhibitors are still administered to selected patients, especially patients with NSCLC and ILA [26, 27].

CT identification of the EGFR mutation status has the potential to inform physicians when tailoring treatment strategies for patients [9, 10]. The clinical characteristics

and CT features of tumors with concurrent ILAs in this study aligned with the findings reported in previous studies that did not consider ILAs [9, 11]. EGFR mutations were more frequently observed in women, non-smokers, early TNM stage, and were associated with a higher frequency of adenocarcinoma. CT features of the EGFR mutation group, compared to the wild-type group, were small tumors, with spiculation, pleural traction, and less pleural fluid. Additionally, fewer tumors were located in the ILA for the EGFR mutant group than in the EGFR wild-type group. The distribution and extent

of ILA findings were analyzed and quantified in detail in this study, this has been discussed less frequently in prior studies. Our results showed that the ILAs of the EGFR mutant group were less distributed in the subpleural zone, and the reticulation score of every zone and the honeycombing score of the middle and lower zones were all significantly lower in the EGFR mutant group than in the wild-type group. Traction bronchiectasis was also less frequently observed in the EGFR mutant group. Multivariable regression analyses demonstrated that the combination of clinical variables, tumor CT features, and ILA CT features significantly improved the predictive ability, with non-fibrotic ILA and small tumors as significant independent predictive factors for EGFR mutation. EGFR mutations occurred less frequently in subpleural fibrotic ILA, a finding that corresponds to previous studies that reported a low prevalence of EGFR mutations in patients with lung cancer and UIP or IPF [12, 24]. Watanabe et al. [28] reported that the origin of lung cancer in the subpleural region was correlated with UIP. Sakuma et al. [29] further demonstrated that alveolar epithelial cells that have undergone epithelial-to-mesenchymal transition (EMT) may contribute to the formation of fibroblastic foci in IPF, whereas EGFR-mutant lung adenocarcinoma cells that have undergone EMT lack EGFR dependency. This may elucidate the potential pathophysiological mechanisms underlying subpleural fibrotic ILA, which is mostly accompanied by wild-type EGFR lung cancer.

Previous studies have demonstrated that the detection of ILA in patients with early or advanced NSCLC is correlated with a decreased OS rate [6, 14, 22]. In addition, subpleural fibrotic ILAs are linked to a lower survival rate than non-fibrotic ILAs [14, 15, 30]; however, EGFR mutation status was not included in these analyses. Researchers have reported EGFR mutations as a good prognostic factor for advanced lung cancer, but not for operable early stage lung adenocarcinoma [8, 11]. In our study, 80.7% of patients were diagnosed with stage III-IV lung cancer, and EGFR mutation status was incorporated into the multivariate analysis and identified as an independent prognostic factor for patients with lung cancer and ILA, after excluding those with subpleural fibrotic ILA. Similarly, Kanaji et al. [24] reported that the lack of EGFR mutations and the presence of IPF were unfavorable prognostic factors for progression-free survival and OS. Given the significantly better prognosis of patients with ILAs compared to those with IPF [4, 15, 24], this may explain why subpleural fibrotic ILA is not an independent prognostic factor. Overall, acknowledging the prognostic implications of EGFR mutations in lung cancer with ILAs can greatly influence clinical decision-making.

This study had several limitations. First, the retrospective nature of this single-center observational study resulted in a natural selection bias and missing data. A prospective study with multicenter data is necessary in the future. Second, due to the low prevalence of EGFR mutations in patients with ILAs, the sample size was relatively small in this study for the EGFR mutation group; however, the association between EGFR mutations and CT features of ILAs is of significant clinical and statistical importance. Third, 78% (85/109) of the patients in the study underwent biopsy procedures to obtain samples, as most patients presented with stage III-IV lung cancer. However, both the adequacy of the sample and accuracy of the diagnosis of EGFR mutations were rigorously confirmed. Finally, the assessment primarily concentrated on the baseline ILA, without further dynamic observation of the ILA or examination of its connection to OS. Future research should involve additional investigations in this area.

Conclusions

The presence of non-fibrotic ILA is associated with an increased incidence of EGFR mutations, whereas the presence of EGFR mutations rather than ILA is an independent positive prognostic factor for patients with NSCLC. Consequently, understanding the predictive significance of ILA for EGFR mutations and the prognostic value of EGFR status can assist clinicians and radiologists in improving their understanding and evaluation of the long-term prognosis of patients with NSCLC and ILAs.

Abbreviations

AUC	Area under the receiver operating characteristic curve
CI	Confidence interval
CT	Computed tomography
EGFR	Epidermal growth factor receptor
GGO	Ground-glass opacity
HR	Hazard ratio
HRCT	High-resolution computed tomography
ILA	Interstitial lung abnormality
ILD	Interstitial lung disease
IPF	Idiopathic pulmonary fibrosis
NSCLC	Non-small cell lung cancer
OS	Overall survival
ROC	Receiver operating characteristic
UIP	Usual interstitial pneumonia

Acknowledgements

We would like to thank Editage (www.editage.cn) for English language editing.

Authors' contributions

(a) Conception and design: Yanli Gao, Yuhui Zhang; (b) Administrative support: Kewu Huang; (c) Provision of study materials or patients: Yanli Gao, Xiaoli Xu, Min Zhu; (d) Collection and assembly of data: Xiaoli Xu, Min Zhu, Jialu Li, Tao Ouyang, Cen Chen; (e) Data analysis and interpretation: Xiaoli Xu, Zixing Wang; (f) Manuscript writing: Xiaoli Xu; (g) Final approval of manuscript: All authors.

Funding

The research was supported by National Natural Science Foundation of China (82000103).

Availability of data and materials

The datasets used and analyzed during the study are available from the corresponding authors on reasonable request.

Declarations**Ethics approval and consent to participate**

This study conformed to the Declaration of Helsinki on Human Research Ethics standards and was approved by the institutional review board of Beijing Chaoyang Hospital of Capital Medical University. The need for written, informed consent was waived because of the retrospective study.

Consent for publication

All authors contributed to the writing of the manuscript and consented to publication.

Competing interests

The authors have no relevant financial or non-financial interests to disclose.

Received: 4 December 2023 Accepted: 11 May 2024

Published online: 23 May 2024

References

- Jin GY, Lynch D, Chawla A, et al. Interstitial lung abnormalities in a CT lung cancer screening population: prevalence and progression rate. *Radiology*. 2013;268:563–71. <https://doi.org/10.1148/radiol.13120816>.
- Washko GR, Hunninghake GM, Fernandez IE, et al. Lung volumes and emphysema in smokers with interstitial lung abnormalities. *N Engl J Med*. 2011;364:897–906. <https://doi.org/10.1056/NEJMoa1007285>.
- Chae KJ, Lim S, Seo JB, et al. Interstitial lung abnormalities at CT in the Korean National Lung Cancer Screening Program: prevalence and deep learning-based texture analysis. *Radiology*. 2023;307: e222828. <https://doi.org/10.1148/radiol.222828>.
- Hatabu H, Hunninghake GM, Richeldi L, et al. Interstitial lung abnormalities detected incidentally on CT: a position paper from the Fleischner Society. *Lancet Respir Med*. 2020;8:726–37. [https://doi.org/10.1016/s2213-2600\(20\)30168-5](https://doi.org/10.1016/s2213-2600(20)30168-5).
- Putman RK, Hatabu H, Araki T, et al. Association between interstitial lung abnormalities and all-cause mortality. *JAMA*. 2016;315:672–81. <https://doi.org/10.1001/jama.2016.0518>.
- Araki T, Dahlberg SE, Hida T, et al. Interstitial lung abnormality in stage IV non-small cell lung cancer: a validation study for the association with poor clinical outcome. *Eur J Radiol Open*. 2019;6:128–31. <https://doi.org/10.1016/j.ejro.2019.03.003>.
- Ramalingam SS, Vansteenkiste J, Planchard D, et al. Overall survival with osimertinib in untreated, EGFR-mutated advanced NSCLC. *N Engl J Med*. 2020;382:41–50. <https://doi.org/10.1056/NEJMoa1913662>.
- Choi CM, Kim MY, Lee JC, Kim HJ. Advanced lung adenocarcinoma harboring a mutation of the epidermal growth factor receptor: CT findings after tyrosine kinase inhibitor therapy. *Radiology*. 2014;270:574–82. <https://doi.org/10.1148/radiol.13121824>.
- Yang X, Liu M, Ren Y, et al. Using contrast-enhanced CT and non-contrast-enhanced CT to predict EGFR mutation status in NSCLC patients—a radiomics nomogram analysis. *Eur Radiol*. 2021. <https://doi.org/10.1007/s00330-021-08366-y>.
- Liu Y, Kim J, Qu F, et al. CT features associated with epidermal growth factor receptor mutation status in patients with lung adenocarcinoma. *Radiology*. 2016;280:271–80. <https://doi.org/10.1148/radiol.2016151455>.
- Yotsukura M, Yasuda H, Shigenobu T, et al. Clinical and pathological characteristics of EGFR mutation in operable early-stage lung adenocarcinoma. *Lung Cancer*. 2017;109:45–51. <https://doi.org/10.1016/j.lungcan.2017.04.014>.
- Masai K, Tsuta K, Motoi N, et al. Clinicopathological, immunohistochemical, and genetic features of primary lung adenocarcinoma occurring in the setting of usual interstitial pneumonia pattern. *J Thorac Oncol*. 2016;11:2141–9. <https://doi.org/10.1016/j.jtho.2016.07.034>.
- Im Y, Chung MP, Lee KS, et al. Impact of interstitial lung abnormalities on postoperative pulmonary complications and survival of lung cancer. *Thorax*. 2023;78:183–90. <https://doi.org/10.1136/thoraxjnl-2021-218055>.
- Ahn Y, Lee SM, Choi S, et al. Automated CT quantification of interstitial lung abnormality and interstitial lung disease according to the Fleischner Society in patients with resectable lung cancer: prognostic significance. *Eur Radiol*. 2023. <https://doi.org/10.1007/s00330-023-09783-x>.
- Putman RK, Gudmundsson G, Axelsson GT, et al. Imaging patterns are associated with interstitial lung abnormality progression and mortality. *Am J Respir Crit Care Med*. 2019;200:175–83. <https://doi.org/10.1164/rccm.201809-1652OC>.
- Nicholson AG, Tsao MS, Beasley MB, et al. The 2021 WHO classification of lung tumors: impact of advances since 2015. *J Thorac Oncol*. 2022;17:362–87. <https://doi.org/10.1016/j.jtho.2021.11.003>.
- Goldstraw P, Chansky K, Crowley J, et al. The IASLC lung cancer staging project: proposals for revision of the TNM stage groupings in the forthcoming (eighth) edition of the TNM classification for lung cancer. *J Thorac Oncol*. 2016;11:39–51. <https://doi.org/10.1016/j.jtho.2015.09.009>.
- Raghu G, Remy-Jardin M, Myers JL, et al. Diagnosis of idiopathic pulmonary fibrosis. an official ATS/ERS/JRS/ALAT clinical practice guideline. *Am J Respir Crit Care Med*. 2018;198:e44–68. <https://doi.org/10.1164/rccm.201807-1255ST>.
- Sumikawa H, Johkoh T, Fujimoto K, et al. Pathologically proved nonspecific interstitial pneumonia: CT pattern analysis as compared with usual interstitial pneumonia CT pattern. *Radiology*. 2014;272:549–56. <https://doi.org/10.1148/radiol.14130853>.
- Xu X, Sui X, Zhong W, et al. Clinical utility of quantitative dual-energy CT iodine maps and CT morphological features in distinguishing small-cell from non-small-cell lung cancer. *Clin Radiol*. 2019;74:268–77. <https://doi.org/10.1016/j.crad.2018.10.012>.
- Axelsson GT, Putman RK, Aspelund T, et al. The associations of interstitial lung abnormalities with cancer diagnoses and mortality. *Eur Respir J*. 2020;56. <https://doi.org/10.1183/13993003.02154-2019>.
- Zhu M, Yi J, Su Y, et al. Newly diagnosed non-small cell lung cancer with interstitial lung abnormality: prevalence, characteristics, and prognosis. *Thorax*. 2023;14:1874–82. <https://doi.org/10.1111/1759-7714.14935>.
- Chapman AM, Sun KY, Ruestow P, Cowan DM, Madl AK. Lung cancer mutation profile of EGFR, ALK, and KRAS: meta-analysis and comparison of never and ever smokers. *Lung Cancer*. 2016;102:122–34. <https://doi.org/10.1016/j.lungcan.2016.10.010>.
- Kanaji N, Tadokoro A, Kita N, et al. Impact of idiopathic pulmonary fibrosis on advanced non-small cell lung cancer survival. *J Cancer Res Clin Oncol*. 2016;142:1855–65. <https://doi.org/10.1007/s00432-016-2199-z>.
- Ichihara E, Miyahara N, Maeda Y, Kiura K. Managing lung cancer with comorbid interstitial pneumonia. *Intern Med*. 2020;59:163–7. <https://doi.org/10.2169/internalmedicine.3481-19>.
- Ando M, Okamoto I, Yamamoto N, et al. Predictive factors for interstitial lung disease, antitumor response, and survival in non-small-cell lung cancer patients treated with gefitinib. *J Clin Oncol*. 2006;24:2549–56. <https://doi.org/10.1200/jco.2005.04.9866>.
- Ogura T, Takigawa N, Tomii K, et al. Summary of the Japanese respiratory society statement for the treatment of lung cancer with comorbid interstitial pneumonia. *Respir Invest*. 2019;57:512–33. <https://doi.org/10.1016/j.resinv.2019.06.001>.
- Watanabe Y, Kawabata Y, Koyama N, et al. A clinicopathological study of surgically resected lung cancer in patients with usual interstitial pneumonia. *Respir Med*. 2017;129:158–63. <https://doi.org/10.1016/j.rmed.2017.06.015>.
- Sakuma Y. Epithelial-to-mesenchymal transition and its role in EGFR-mutant lung adenocarcinoma and idiopathic pulmonary fibrosis. *Pathol Int*. 2017;67:379–88. <https://doi.org/10.1111/pin.12553>.
- Iwasawa T, Okudela K, Takemura T, et al. Computer-aided quantification of pulmonary fibrosis in patients with lung cancer: relationship to disease-free survival. *Radiology*. 2019;292:489–98. <https://doi.org/10.1148/radiol.2019182466>.

Publisher's Note

Springer Nature remains neutral with regard to jurisdictional claims in published maps and institutional affiliations.